CHEMISTRY OF MATERIALS
Article

Chem. Mater. **2010,** *22,* 5199–5208 5199
DOI:10.1021/cm101151n

Effect of Alumina Release Rate on the Mechanism of Geopolymer Gel Formation

Ailar Hajimohammadi,[†] John L. Provis,*[,†] and Jannie S. J. van Deventer[†,‡]

[†]*Department of Chemical and Biomolecular Engineering, University of Melbourne, Victoria 3010, Australia, and* [‡]*Zeobond Pty. Ltd., P.O. Box 210, Somerton, Victoria 3062, Australia*

Received April 24, 2010. Revised Manuscript Received August 10, 2010

The effect of the rate of alumina release during the reaction of a one-part (just-add-water) geopolymer mix on growing geopolymer gels is investigated by coupling time-resolved and spatially resolved infrared spectroscopic analysis. The rate of alumina release from different precursors has previously been identified as a critical controlling factor in the formation of mechanically strong and durable geopolymers; however, its influence on the nanostructure of the geopolymer gel has never before been directly analyzed. Gel microstructure and nanostructure are able to be observed by synchrotron radiation-based infrared microscopy (SR-FTIR) with hierarchical clustering analysis, conducted in conjunction with the in situ attenuated total reflectance (ATR) FTIR technique to provide temporal resolution. The SR-FTIR technique provides the opportunity to analyze the chemistry of the heterogeneous geopolymer binder at a level of detail that previously has not been available. Although spatially averaged (ATR-FTIR) infrared results show similar spectra for well-cured samples with different alumina release rates, SR-FTIR shows that the gels are markedly different, with less unreacted silica particles remaining in geopolymer gels with slow alumina release, but greater homogeneity when alumina is released more rapidly. Rapid release of alumina is shown to impede the dissolution of silica particles in the early stages of the reaction; thus, the participation of alumina in forming geopolymer gels appears to be more beneficial to geopolymer nanostructural development when it becomes available in the later stages of the reaction process.

1. Introduction

Hardened alkali-activated aluminosilicate gels containing Si−O−Si and Si−O−Al bonds in a highly cross-linked X-ray amorphous network have become known as "geopolymers",[1] and these materials show significant potential in construction applications as an alternative to portland cement. Geopolymers do show some performance advantages, compared to traditional construction materials; however, it is the possibility of considerable savings in greenhouse gas emissions as a cement replacement material[2,3] that has accelerated scientific interest in these materials in recent years.

Although geopolymer technology is now finding commercial application in civil infrastructure applications,[4] a more complete understanding of the chemistry responsible for the formation and hardening of the gel is critical to the widespread acceptance of these binders. A variety of analytical techniques have been applied to satisfy the need to understand and control geopolymer behavior, and the ability to tailor binder formulations to optimize specific properties is increasing; however, much about these materials is still not well understood.[5−8]

Generally, an aluminosilicate source (such as fly ash or metakaolin), an alkali metal hydroxide or alkali silicate source, and water (to enable mixing and mediate the reaction) are required for the synthesis of geopolymers. According to the generally accepted reaction sequence of geopolymerization,[5,9] the first stage of reaction is the release of aluminate and silicate monomers by alkali attack on the solid aluminosilicate source, which is required for the conversion of solid particles to geopolymer gel.[10] Hydrolysis reactions occur on the surface of the solid particles, followed by the formation of dissolved species that cross-link to form oligomers, and then setting and hardening are attributed to polycondensation and the formation of a three-dimensional aluminosilicate network.[11]

*Author to whom correspondence should be addressed. Phone: +61 3 8344 8755. Fax: +61 3 8344 4153. E-mail: jprovis@unimelb.edu.au.

(1) Davidovits, J. *J. Therm. Anal. Calorim.* **1991**, *37*, 1633.
(2) Gartner, E. *Cem. Concr. Res.* **2004**, *34*, 1489.
(3) Duxson, P.; Provis, J. L.; Lukey, G. C.; van Deventer, J. S. J. *Cem. Concr. Res.* **2007**, *37*, 1590.
(4) van Deventer, J. S. J.; Provis, J. L.; Duxson, P.; Brice, D. G. *Waste Biomass Valorization* **2010**, *1*, 145.
(5) Duxson, P.; Fernández-Jiménez, A.; Provis, J. L.; Lukey, G. C.; Palomo, A.; van Deventer, J. S. J. *J. Mater. Sci.* **2007**, *42*, 2917.
(6) Provis, J. L.; Lukey, G. C.; van Deventer, J. S. J. *Chem. Mater.* **2005**, *17*, 3075.
(7) Duxson, P.; Provis, J. L. *J. Am. Ceram. Soc.* **2008**, *91*, 3864.
(8) Provis, J. L., van Deventer, J. S. J., Eds. *Geopolymers: Structure, Processing, Properties and Industrial Applications*; Woodhead: Abington, U.K., 2009.
(9) Rees, C. A.; Provis, J. L.; Lukey, G. C.; van Deventer, J. S. J. *Langmuir* **2007**, *23*, 8170.
(10) Provis, J. L.; van Deventer, J. S. J. *Chem. Eng. Sci.* **2007**, *62*, 2318.
(11) Fernández-Jiménez, A.; Palomo, A.; Sobrados, I.; Sanz, J. *Microporous Mesoporous Mater.* **2006**, *91*, 111.

© 2010 American Chemical Society
Published on Web 08/25/2010

Reaction conditions, raw material characteristics,[12] and the nature and concentration of alkali cations added,[13,14] are known to affect the chemical and microstructural arrangement of silicon and aluminum in the geopolymer gel network and, consequently, the physical and chemical properties of the final binder. The rates of the release of silicate and aluminate species are very important in controlling the conversion of starting materials and the development of geopolymer gel. A high early dissolved silicate concentration is known to accelerate the conversion of aluminosilicate materials to geopolymer,[11,15] while the availability of aluminum in the starting materials, and the rate of its release, are also known to control geopolymer gel properties.[11,15] However, in traditional geopolymer-forming systems utilizing a solid aluminosilicate precursor such as metakaolin or fly ash, the release rates of silica and alumina cannot be decoupled from each other, because the two elements are supplied by dissolution of the same solid precursor. The development of a one-part, "just add water" geopolymer system,[16] where the geopolymer gel is obtained by mixing a reactive silica powder (commonly geothermal silica, which is a waste product from geothermal power generation) with solid alkali and alumina sources (which may be combined as solid sodium aluminate, or may be separate) provides the opportunity to decouple the elemental release rates. This enables more-detailed analysis of the distinct effects of silica and alumina in the early and later stages of geopolymer gel formation.

Two different aluminosilicate gel phases are known to develop consecutively in a low-calcium fly ash geopolymer system;[11,17] however, the factors that control phase development and the process of transformation into the final binder are not yet well understood. In Fourier transform infrared (FTIR) spectroscopy studies of geopolymer systems, the main Si−O−T (where T is tetrahedral Si or Al) asymmetric stretching band is very important, because it carries information about the Si/Al ratios and connectivity of developing geopolymer gels.[9,13,18,19] However, it has never before been possible to analyze the spatial distribution of gel connectivity within the geopolymer binder, because all available FTIR information regarding geopolymer formation mechanisms relies on spatially averaged results.

On a length scale of nanometers to micrometers, geopolymers are well-known to be heterogeneous,[5,6,20−22] but the nature of this heterogeneity is still not fully understood.[9,13,23] Recently, synchrotron X-ray fluorescence has been utilized for the analysis of heterogeneous fly ash geopolymers, using a hard X-ray nanoprobe instrument with high spatial resolution (30 nm),[24] which provided detailed elemental distribution data but not spectroscopic information regarding Si/Al structures within the geopolymer gel. Spatially resolved spectroscopy with sensitivity to Si/Al bonding environments is an area that provides significant experimental challenges; however, advances in synchrotron-based instrumentation are now providing the opportunity for significant progress in this area.

Here, we present the results of an investigation of the effects of the rate of release of alumina from geopolymer precursors. For the first time, synchrotron radiation-based infrared microscopy (SR-FTIR) is utilized to study geopolymeric materials, and the results of time-resolved and spatially resolved FTIR data are correlated. Preliminary SR-FTIR studies have shown very promising results regarding understanding the geopolymerization reaction mechanism by investigation of inhomogeneous samples.[25]

The main objective of this paper is to describe the effect of alumina release rate on the mechanism of geopolymer gel formation. The SR-FTIR technique is applied in conjunction with complementary methods of analysis, to better understand the chemistry of geopolymer gels and, in particular, the inter-relationship between kinetics and the spatial distribution of bonding environments. Although the samples with different rates of alumina release show very similar spatially averaged FTIR spectra after three weeks of curing, SR-FTIR clearly shows that the rate of alumina release influences the degree of homogeneity of the geopolymer gel, and this can have consequences for geopolymer performance in applications requiring high durability and strength.

2. Materials and Methods

As a source of reactive silica and alumina, fly ash (reactive components: 36.6% amorphous SiO_2 and 15.3% amorphous Al_2O_3; the remainder is unreactive crystalline mullite, quartz, and iron oxide phases) sourced from Gladstone Power Station, Queensland, Australia,[13] as well as washed, dried, and milled geothermal silica (96% SiO_2, Cerro Prieto geothermal power station, Mexico[16]) were mixed at a ratio of 1.5 g fly ash per gram of geothermal silica. Two geopolymer sample formulations were made from the

(12) Duxson, P.; Provis, J. L.; Lukey, G. C.; Separovic, F.; van Deventer, J. S. J. *Langmuir* **2005**, *21*, 3028.
(13) Rees, C. A.; Provis, J. L.; Lukey, G. C.; van Deventer, J. S. J. *Langmuir* **2007**, *23*, 9076.
(14) Lee, W. K. W.; van Deventer, J. S. J. *Colloids Surfaces A* **2002**, *211*, 49.
(15) De Silva, P.; Sagoe-Crentsil, K.; Sirivivatnanon, V. *Cem. Concr. Res.* **2007**, *37*, 512.
(16) Hajimohammadi, A.; Provis, J. L.; van Deventer, J. S. J. *Ind. Eng. Chem. Res.* **2008**, *47*, 9396.
(17) Fernández-Jiménez, A.; de la Torre, A. G.; Palomo, A.; López-Olmo, G.; Alonso, M. M.; Aranda, M. A. G. *Fuel* **2006**, *85*, 1960.
(18) Lee, W. K. W.; van Deventer, J. S. J. *Langmuir* **2003**, *19*, 8726.
(19) Fernández-Jiménez, A.; de la Torre, A. G.; Palomo, A.; Lopez-Olmo, G.; Alonso, M. M.; Aranda, M. A. G. *Fuel* **2006**, *85*, 625.
(20) Lloyd, R. R.; Provis, J. L.; van Deventer, J. S. J. *J. Mater. Sci.* **2009**, *44*, 608.
(21) Lloyd, R. R.; Provis, J. L.; van Deventer, J. S. J. *J. Mater. Sci.* **2009**, *44*, 620.
(22) Duxson, P.; Provis, J. L.; Lukey, G. C.; Mallicoat, S. W.; Kriven, W. M.; van Deventer, J. S. J. *Colloids Surf. A* **2005**, *269*, 47.
(23) van Deventer, J. S. J.; Provis, J. L.; Duxson, P.; Lukey, G. C. *J. Hazard. Mater.* **2007**, *139*, 506.
(24) Provis, J. L.; Rose, V.; Bernal, S. A.; van Deventer, J. S. J. *Langmuir* **2009**, *25*, 11897.
(25) Hajimohammadi, A.; Provis, J. L.; van Deventer, J. S. J. Using synchrotron radiation Fourier transform infrared microscopy to investigate the effect of timed release of aluminate during geopolymer gel formation. In *2nd International Congress on Green Process Engineering* (*GPE 2009*), Venice, Italy, June 14−17, 2009. (CD-ROM proceedings.)

Table 1. Amount of Each Component in the Samples Studied in This Work

	Composition (wt %)					
sample	fly ash	geothermal silica	sodium hydroxide	amorphous alumina	sodium aluminate	water
A	26.5	17.9	12	11.1	0	32.5
B	26.7	18	1.4	0	20.1	33.8

resulting mixture by adding different alumina sources: one using sodium aluminate (Aldrich; 55.2 wt % Al_2O_3 and 42.7 wt % Na_2O) and the other with amorphous alumina (BET surface area = 62.6 m^2/g) synthesized via the Sims and Bingham method.[16,26] Milled sodium hydroxide pellets are also used to enable the matching of Na/Al ratios between samples.

Both sample formulations have molar ratios of Si/Al = 1.5, Na/Al = 1, and H_2O/Na_2O = 12; Table 1 shows the sample formulations on a mass basis, where the water content was adjusted to account for the small amount of water present in NaOH pellets. Therefore, except for the rate of release of alumina, which is markedly faster in the sample containing sodium aluminate, other compositional parameters are kept similar. The sample with slow alumina release (containing amorphous alumina) is called sample A, and the sample with faster alumina release is called sample B. Geopolymer pastes were cured at 40 °C in an oven after mixing.

X-ray diffraction (XRD) (Phillips PW-1800) was conducted using Cu Kα X-ray irradiation, 30 mA and 40 kV, with 0.02° 2θ steps, 2 s $step^{-1}$. Attenuated total reflectance Fourier-transform infrared (ATR-FTIR) spectra were collected using a Varian FTS 7000 FT-IR spectrometer, with a Specac MKII Golden Gate single reflectance diamond ATR attachment with KRS-5 lenses and heater top plate. Absorbance spectra were collected from 4000 cm^{-1} to 400 cm^{-1} at a resolution of 2 cm^{-1} and a scanning speed of 5 kHz, with 32 scans. For in situ studies, geopolymer pastes were mounted on the ATR crystal immediately after mixing, and the sample holder was sealed to avoid any loss of water. The hot plate temperature was maintained at 40 °C to provide the same environment as the curing oven, and the FTIR spectra were collected every minute.

Spatially resolved FTIR spectra (SR-FTIR) were obtained using the microscopy endstation on BL8 (infrared spectroscopy) at the Australian Synchrotron, Melbourne. Samples were cut with a diamond saw and polished to a 6 μm diamond paste finish, using the same polishing technique as that applied elsewhere for the electron microscopic analysis of geopolymers.[20] Using the attached optical microscope, a region of interest was defined on each sample as a rectangle 30 × 20 points in size, on 10 μm grid spacing. A 20 μm × 20 μm aperture size was used. After defining these positions, the ATR crystal was moved to these points and FTIR data were collected (64 scans per spot, from 3000 cm^{-1} to 700 cm^{-1}). Two regions on each sample were studied, and the consistency of the results was checked.

The hierarchical clustering analysis (HCA) method was applied to analysis of the SR-FTIR data using the CytoSpec software. Baselines were corrected to set a straight baseline for the regions with no peaks. Then, the collected FTIR spectra were cut from wavenumbers of 800 cm^{-1} to 1200 cm^{-1}, and normalized using the vector normalization method. Finally, smoothing was applied to the entire region, using the average smoothing algorithm, as implemented in the Cytospec software.

The mechanical strength of geopolymers was measured using 50-mm mortar cubes. Geopolymer pastes were mixed with a standard sand in the proportion of 2 g of sand per gram of geopolymer, molded, sealed, and cured in an oven at 40 °C. Strengths reported are the average of three samples.

3. Results and Discussion

3.1. Characterizing Crystalline Phases. XRD results for samples A and B cured at 40 °C for 3 months are presented in Figure 1. The main crystalline phases observed in the samples are quartz (SiO_2, Joint Committee on Powder Diffraction Standards (JCPDS) File Card No. 01-079-1906), mullite (approximately $Al_6Si_2O_{13}$, JCPDS File Card No. 00-015-0776), two forms of faujasite (F1 (approximately $Na_2Al_2Si_4O_{12}\cdot 8H_2O$, JCPDS File Card No. 00-039-1380) and F2 (approximately $Na_2Al_2Si_{2.4}O_{8.8}\cdot 6.7H_2O$, JCPDS File Card No. 00-012-0246); these are distinguishable from each other as the lattice parameter of faujasite varies with Si/Al content,[27] which enables the use of XRD to obtain some compositional information) and hydroxysodalite ($Na_6(AlSiO_4)_6\cdot 4H_2O$, JCPDS File Card No. 00-042-0216). Iron oxides, mostly in the form of a ferrite spinel (Fe_3O_4 with substitution of various elements onto both Fe^{2+} and Fe^{3+} sites),[24] are also present in both samples. Quartz, mullite, and iron oxides are the main crystal phases present in Gladstone fly ash[18,28] and are largely unaffected by the geopolymerization process. The amount of faujasite formed in sample B, with more rapid alumina release, is much less than that in sample A, and the crystallites also seem to be very small in this case, because of the broad peaks in the diffractogram. Consistent with the majority of the geopolymers literature,[6] the hump from 20° 2θ to 40° 2θ in both samples demonstrates that a significant amount of the geopolymer gel is X-ray amorphous.

Figure 1 shows obvious differences in the degree of crystallinity and in the crystal phases formed in the two samples. As the formation from a gel of new zeolites with Si/Al ratio close to that of the surrounding gel shows a lower activation energy,[29] the compositions of these

(26) Sims, J. R.; Bingham, F. T. *Soil Sci. Soc. Am. J.* **1968**, *32*, 364.
(27) Dempsey, E.; Kühl, G. H.; Olson, D. H. *J. Phys. Chem.* **1969**, *73*, 387.
(28) Phair, J. W.; van Deventer, J. S. J.; Smith, J. D. *Appl. Geochem.* **2004**, *19*, 423.
(29) Barrer, R. M.; Mainwaring, D. E. *J. Chem. Soc.: Dalton Trans.* **1972**, 2534.

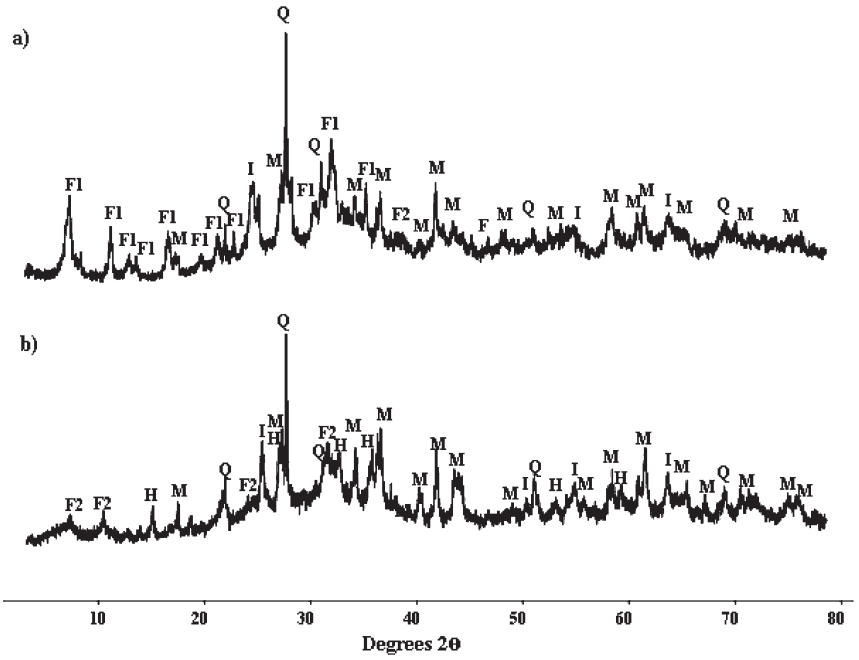

Figure 1. XRD diffractograms of (a) sample A and (b) sample B, cured at 40 °C for 3 months. F1 and F2 represent two different forms of faujasite ($Na_2Al_2Si_4O_{12}\cdot 8H_2O$ and $Na_2Al_2Si_{2.4}O_{8.8}\cdot 6.7H_2O$, respectively); H, hydroxysodalite ($Na_6(AlSiO_4)_6\cdot 4H_2O$); Q, quartz ($SiO_2$); M, mullite ($Al_6Si_2O_{13}$); and I, iron oxide ($Fe_3O_4$).

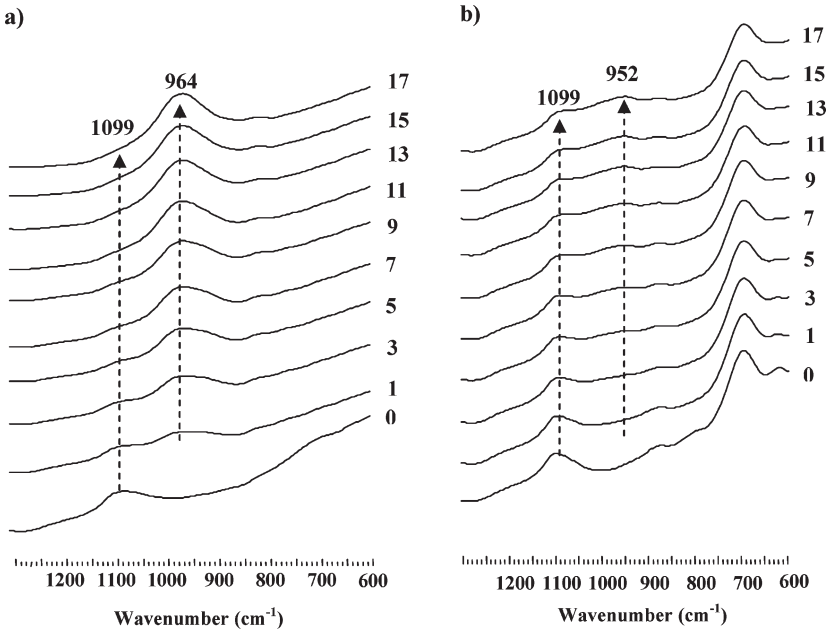

Figure 2. Selected in situ ATR-FTIR spectra of (a) sample A and (b) sample B, as a function of reaction time. Numbers alongside each spectrum refer to the age of samples in hours and arrows mark key peak positions; the spectra shown are representative of the complete dataset, which was obtained at a rate of one scan per minute.

crystal phases can be used to provide some indication of the local composition of the geopolymer gel. Although both total mix compositions were the same, more faujasite crystals appeared in sample A and with an Si/Al molar ratio of ~2 (phase F1), while fewer faujasite crystals formed in sample B and with an Si/Al molar ratio of ~1.2 (phase F2). Also, hydroxysodalite with an Si/Al molar ratio of 1 is only formed in sample B.

The formation of higher Si/Al ratio crystals in sample A, with its slower alumina release rate, can be attributed to the lower availability of aluminum in this sample, which provides a suitable environment for the formation of crystal phases with higher silicon content. This may also suggest that the surrounding gels are very likely to have corresponding differences in composition, although this point will be revisited in detail later in this paper, through the use of the SR-FTIR technique.

3.2. Gel Network Structure Analysis. The reaction processes that occur in the two geopolymer formulations with different rates of alumina release were studied using in situ ATR-FTIR (Figure 2). Figure 2 shows that the chemical changes that occur in the two samples are very

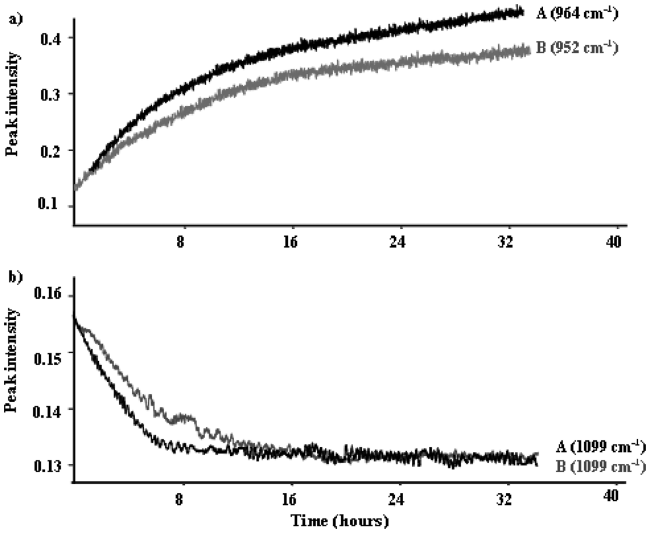

Figure 3. Functional group analysis of (a) geopolymer and (b) unreacted silica peaks (plotting the intensity of FTIR peaks as a function of curing time) in samples A and B, from in situ ATR-FTIR spectra.

different, from the beginning of the reaction. The large band at ~710 cm^{-1} in sample B is related to the Al−O vibrations of sodium aluminate,[30] and its intensity decrease indicates a reduction in the amount of free aluminate over time. Comparison of the intensity of the 1100 cm^{-1} band, which is attributed to Si−O−Si vibrations of unreacted geothermal silica and quartz, with the intensity of the 950−960 cm^{-1} band, which is due to Si−O−Si and Si−O−Al vibrations of the growing geopolymeric gels, provides information about the extent of the reaction in the early stages of formation of fly ash geopolymers.[9,16,31]

Figure 3 presents a functional group analysis showing the change in intensity, as a function of time, at the positions marked with arrows in Figure 2; this is similar to the type of analysis that has been presented previously for fly ash geopolymer systems.[13] Using a high-alkalinity mix design (Na/Al molar ratio of 1) and adding highly soluble geothermal silica seems to remove the induction period that is sometimes observed in fly ash geopolymers, particularly when hydroxide activation is used.[9] It is also evident from these plots that sample B shows slower changes in its structure than does sample A, even though the release rate of alumina in sample B is higher. In particular, sample A shows more rapid initial silica dissolution from raw materials (although similar final intensities for this wavenumber are observed in the two samples) in Figure 3b, and a greater extent of formation of the new geopolymer gel in Figure 3a.

These results suggest that, in the first few hours after mixing, the changes in chemical structure of the gel product are happening much more rapidly in the sample with a slow alumina release rate (sample A), compared to the changes in the fast alumina release sample (sample B). This indicates that the rapid initial release of alumina limits the dissolution of silica particles at the beginning of the reaction. It is well-known that the presence of soluble aluminum considerably reduces the solubility of silica in water.[32,33] The aqueous Al species readily available in

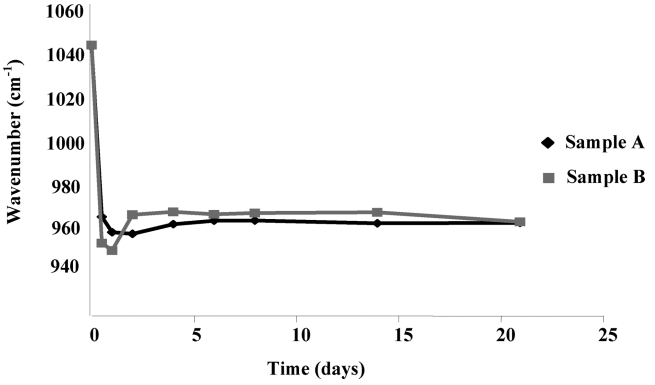

Figure 4. Position of the peak maximum in the Si−O−(Si,Al) asymmetric stretch region for samples A and B, as a function of curing time, from in situ (less than 1 day) and ex situ (3−21 days) ATR-FTIR spectra.

sample B adsorb onto the surface of undissolved silica, which hinders the dissolution process in this sample.[34−36]

The position of the main Si−O−T band, as a function of reaction time, carries vital information about the formation and structure of the growing geopolymer gel, as shown in Figure 4.

The asymmetric stretch of unreacted geothermal silica occurs at ~1100 cm^{-1} in the as-mixed slurry; the main fly ash glass peak (~1055 cm^{-1} for this fly ash from previous work[9,13]) is not evident here when the fly ash is blended with geothermal silica. A shift in this band to lower wavenumbers means that some changes are occurring in the length and angle of the Si−O−T bonds in the gel.[37] The changes that cause a decrease in wavenumber can either be an increase in the concentration of nonbridging oxygens (NBOs),[38] or more substitution of Al into the silicate network.[9,18,19] In two systems with the same alkalinity, as studied here, it is unlikely that the main band shift would be due to higher NBO content, because this relates directly to the availability of alkalis, and so the effect observed here is attributed to a higher degree of Al participation in the forming gels.

It is known that when the initial (usually described as "Al-rich"[9,18,19]) aluminosilicate gel begins to form in the early stages of the geopolymerization reaction, the main Si−O−T band shifts to lower wavenumber, and then gradually, with the participation of more silica in older geopolymer gels and an increase in cross-linking, this band usually shifts back to higher wavenumbers. Comparison of the final position of the main band has been used to analyze the extent of Al participation in geopolymer gel structures,[31] and the time when the minimum in

(30) Watling, H. *Appl. Spectrosc.* **1998**, *52*, 250.
(31) Rees, C. Mechanisms and Kinetics of Gel Formation in Geopolymers, Ph.D. Thesis; University of Melbourne: Melbourne, Australia, 2007.
(32) Iler, R. K. *J. Colloid Interface Sci.* **1973**, *43*, 399.
(33) Gasteiger, H. A.; Frederick, W. J.; Streisel, R. C. *Ind. Eng. Chem. Res.* **1992**, *31*, 1183.
(34) Oelkers, E. H.; Gislason, S. R. *Geochim. Cosmochim. Acta* **2001**, *65*, 3671.
(35) Rees, C. A.; Provis, J. L.; Lukey, G. C.; van Deventer, J. S. J. *Colloids Surf. A* **2008**, *318*, 97.
(36) Bickmore, B. R.; Nagy, K. L.; Gray, A. K.; Brinkerhoff, A. R. *Geochim. Cosmochim. Acta* **2006**, *70*, 290.
(37) Innocenzi, P. *J. Non-Cryst. Solids* **2003**, *316*, 309.
(38) Sweet, J. R.; White, W. B. *Phys. Chem. Glasses* **1969**, *10*, 246.

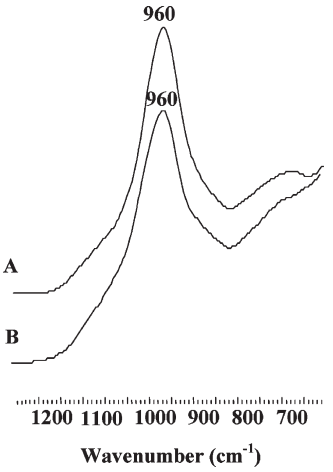

Figure 5. Ex situ ATR-FTIR spectra obtained after 3 weeks of curing at 40 °C, for samples A and B.

peak position occurs has been used to compare the reaction rates of different samples.[31]

Although the time dependence of the position of the main Si−O−T band confirms that there are significant differences between the two samples in the first two days of reaction (Figure 4), these bands shift closer to each other with extended curing, and, finally, after three weeks, the band is present at ~960 cm^{-1} for both samples. The minimum in wavenumber is observed at different times in the two samples; the main band in sample B (with early alumina availability) shifts rapidly to 946 cm^{-1} within the first day and then back to 963 cm^{-1} on the second day, while, in the slow alumina release sample (sample A), the minimum is observed after three days, and is observed at a significantly higher wavenumber (956 cm^{-1}).

With more aqueous alumina available in the solution in the early stages of reaction, the initially formed gel in the sodium aluminate-containing sample B contains more alumina, meaning that the main band shifts to lower wavenumbers. However, after one day, there is now enough dissolved silica released to take part in the reaction and become incorporated into the gel structure, meaning that the main band shifts back to higher wavenumbers. Conversely, the slower release of aluminate species from the precipitated alumina in sample A allows relatively more silica participation in the initial "Al-rich" gel, and, consequently, the band position remains at relatively higher wavenumbers. This initial gel is also more stable than the very Al-rich phase formed in sample B, and therefore shows less variation in peak position after the minimum. The final positions of these bands after 3 weeks of curing are similar at ~960 cm^{-1} for both samples, as shown in Figure 5.

In Figure 5, the spatially averaged ATR-FTIR results indicate that, although the two geopolymer formulations studied here show distinctly different reaction processes in the early stages of reaction, they eventually converge to a similar average gel structure. The greater degree of crystallinity observed in the XRD results is not visible in the infrared spectra, because the quantity of faujasite present is not sufficient to enable the observation of a change in the intensity of its characteristic infrared peaks. If the position and intensity of the Si−O−T asymmetric stretch band are the main points for analysis of geopolymer binders using standard FTIR techniques, Figure 5 shows that the two geopolymer gels are similar in nature on a spatially averaged basis after three weeks of curing. Additional data obtained after 3 months show that both spectra remain essentially unchanged after this curing duration also.

3.3. Spatially Resolved Infrared Spectroscopy. The discussion presented in Section 3.2 provides useful time-resolved information regarding the formation of geopolymer gel, but ATR-FTIR presents only spatially averaged spectra from the sample surface. There is therefore a need for a technique with higher spatial resolution to be able to track chemical events spatially in heterogeneous samples such as geopolymers, and SR-FTIR is a technique that provides such spatial resolution. Some limitations do exist in the resolution of the SR-FTIR technique, as the highest resolution achievable with this wavelength of radiation will provide information averaged over a length scale larger than the fundamental nanoscopic particle size of geopolymer gels. In addition, the penetration depth of infrared radiation into the samples, which is a function of experimental parameters such as the sample material, will set some restrictions on the capabilities of this technique to providing single-peak spectra that could totally differentiate raw materials from geopolymer gels. However, in comparison to the previously available FTIR analysis of the nanostructure of geopolymers, the results of SR-FTIR provide the opportunity for significant progress in this area.

Synchrotron radiation FTIR spectroscopy is applied here for the first time to investigate the effects of timed release of alumina from geopolymer precursor materials. The data are processed by applying hierarchical clustering analysis (HCA), which has been successfully used in different fields of research to analyze and classify collections of complex datasets,[39−42] but never previously applied to the analysis of infrared microscopy data in the study of inorganic gels or in construction materials research. By classifying datasets into a number of clusters, depending on their similarities, this technique aids in data interpretation.

To define the clusters in the HCA method, a distance matrix is first calculated that contains information about the similarities of the spectra. The Cytospec software package is used to conduct this analysis, and the distance matrix calculated using the "D values" method. Pearson's

(39) Helm, D.; Labischinski, H.; Schallehn, G.; Naumann, D. *J. Gen. Microbiol.* **1991**, *137*, 69.
(40) Matthäus, C.; Bird, B.; Miljković, M.; Chernenko, T.; Romeo, M.; Diem, M. Infrared and Raman Microscopy in Cell Biology. *Methods Cell Biol.* **2008**, *89*, 275−308.
(41) Diem, M.; Romeo, M.; Boydston-White, S.; Miljkovi, M.; Matthäus, C. *Analyst* **2004**, *129*, 880.
(42) Bird, B.; Bedrossian, K.; Laver, N.; Miljkovi, M.; Romeo, M. J.; Diem, M. *Analyst* **2009**, *134*, 1067.

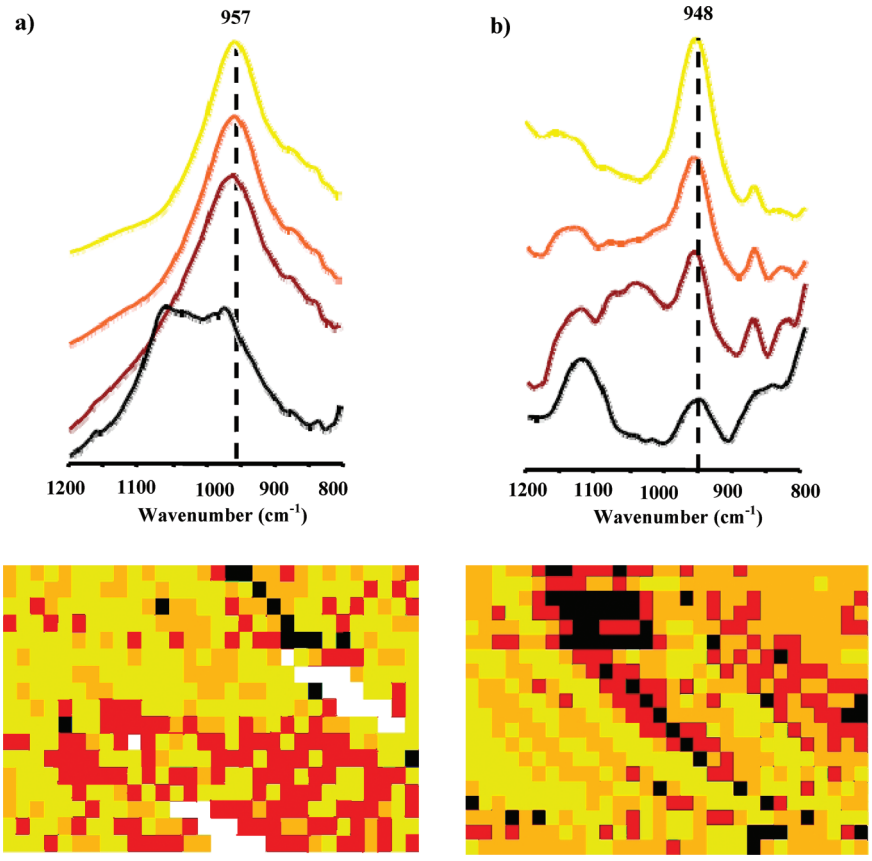

Figure 6. Data from spatially resolved FTIR spectroscopic analysis of samples A and B after 21 days of curing. Hierarchical clusters of (a) sample A and (b) sample B are color-coded and mapped on an HCA image, and the average FTIR spectrum of each cluster is calculated and plotted with the same color. The white areas represent regions where the ATR crystal could not make good contact with the sample, because of polishing scratches. Dashed lines show the wavenumbers of the main bands.

correlation coefficient ($r_{y_1y_2}$) is used to calculate the differences and similarities among the spectra:[43,44]

$$r_{y_1y_2} = \frac{\sum_{i=1}^{n} y_{1i}y_{2i} - n\overline{y_1y_2}}{\sqrt{\sum_{i=1}^{n} y_{1i}^2 - \overline{ny_1}^2}\sqrt{\sum_{i=1}^{n} y_{2i}^2 - \overline{ny_2}^2}} \quad (1)$$

where n is the number of spectra, y_{1i} and y_{2i} are the absorbances of two spectra that are being compared at wavelength i, and $\overline{y_1}$ and $\overline{y_2}$ are the average absorbances of y_1 and y_2. The distinction index $D_{y_1y_2} = 1000(1 - r_{y_1y_2})$ is then calculated.

Finally, cluster analysis is performed using Ward's algorithm.[43−45] The minimum distance between any pair of spectra is first calculated using $D_{y_1y_2}$, so the most similar spectra are identified and combined into one object (cluster). Next, the distances between all spectra are recalculated, considering the new cluster as a single spectrum, and, again, the most similar spectra combined to form a new cluster. These calculations continue until the minimum possible number of clusters is obtained, while retaining enough clusters to enable satisfactory representation of all spectra.[44,46] Selection of the number of clusters depends on the heterogeneity of the sample, and four clusters per sample was determined to be the optimal number here.

Figure 6 demonstrates the outcomes of spatially resolved infrared HCA analysis of the two geopolymer samples with different rates of alumina release.

Although spatially averaged FTIR spectroscopy, as presented in Section 3.2 above, shows the apparently similar nature and behavior of these two different geopolymer mixes after 21 days, the SR-FTIR technique with high spatial resolution presents a different story. In sample A, three of the clustered spectra appear quite similar, with the main band at ~957 cm^{-1} and a small shoulder at 1100 cm^{-1} in each. However, the fourth spectral cluster (shown in black) is markedly distinct from the others, with two strong bands: one close to 1100 cm^{-1} and the other close to 957 cm^{-1}. In sample B, four clearly different spectra could be recognized. Three bands with different intensities are obvious in these spectra, located at 1100, 1050, and 948 cm^{-1}.

This is the first time that time-resolved and spatially resolved FTIR data have been able to be brought together in the analysis of geopolymers, and by comparing the results of the two techniques, it is possible to discover

(43) Hu, X.; Qiu, Z.; Wang, Y.; She, Z.; Qian, G.; Ren, Z. *Bioelectromagnetics* **2009**, *30*, 500.
(44) *CytoSpec Program Documentation*; CytoSpec, Inc.: Boston, MA.
(45) Dziuba, B.; Babuchowski, A.; Nalecz, D.; Niklewicz, M. *Int. Dairy J.* **2007**, *17*, 183.
(46) Yu, P. *J. Agric. Food Chem.* **2005**, *53*, 7115.

important differences in local chemistry of geopolymer gels with different alumina release characteristics.

In situ ATR-FTIR shows that the band at ~1100 cm^{-1}, which is related to Si−O−Si vibrations of unreacted silica particles (mainly geothermal silica[31]), decreases as the reaction proceeds. Finally, after extended reaction time, this band remains only as a small shoulder in the spatially averaged spectra. The main Si−O−Si band in fly ash is known to occur at ~1050 cm^{-1}.[9,17] Therefore, in the spatially resolved data, the regions in which these bands are observed should also be attributed to unreacted silica particles embedded in the geopolymer gel. The particle size of geothermal silica is much smaller than the spatial resolution of SR-FTIR, so these particles would be expected to be observed as a component of a spectrum rather than as a distinct and discrete cluster in the HCA process.

The final Si−O−T band position in the ATR-FTIR spectra after 21 days (the same age as the SR-FTIR samples) was almost identical for both samples studied, at ~960 cm^{-1}. Therefore, the bands at 957 cm^{-1} in sample A and the bands at 948 cm^{-1} in sample B in the HCA cluster spectra also should be related to geopolymer gel.

However, the difference between these peak positions and the ATR-FTIR peak position indicates that the 960 cm^{-1} peaks observed in the two samples are, in fact, due to the superposition of the actual gel peaks (at lower wavenumber) with a higher wavenumber component, which overlaps the gel peak to a sufficient extent to cause its apparent maximum to move to 960 cm^{-1} in both cases. The most likely possible cause for this would be a peak due to one or more phases present in the unreacted fly ash; mullite in particular shows a broad feature in this region,[47] as do some of the aluminosilicate glasses present. Several of the HCA cluster spectra in Figure 6 show significant intensity in this region, so it is apparent that the SR-FTIR analysis enables separation of peak components that are not able to be distinguished in ATR-FTIR spectra. This is important in the correct interpretation of the peak positions in terms of Si/Al ratios, because the SR-FTIR analysis has demonstrated that the gel compositions of the two samples are, in fact, markedly different by enabling separation of these spectral components, which was not possible in the spatially averaged spectra.

The regions related to the black spectrum in sample A (which comprise only a small proportion of the sample) are those with a high amount of unreacted silica, and the rest of the sample is comprised of well-reacted geopolymer gel with a low concentration of intimately intermixed unreacted particles. The main peak position, 957 cm^{-1}, suggests the participation of more Si in the bulk geopolymer gel than is the case in sample B, which has the main band at a lower wavenumber (948 cm^{-1}). These findings confirm the differences between gel chemistry as proposed on the basis of the crystalline phases recognized by XRD, where the formation of higher Si/Al ratio faujasite in sample A suggested a higher gel Si/Al ratio.

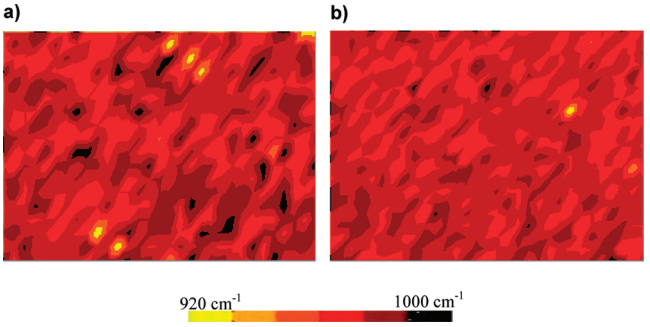

Figure 7. Peak position maps for the 920−1000 cm^{-1} region for (a) sample A and (b) sample B. The color black represents areas with the main band position close to 1000 cm^{-1} and the color yellow shows regions with the main band position closer to 920 cm^{-1}. The presence of more regions with colors close to the limiting borders (yellow or black) indicates a wider distribution of main peak positions.

Comparing the two maps in Figure 6, the regions with high amount of unreacted siliceous materials (black and brown spectra) are much more prominent in sample B than the corresponding regions in sample A (black spectrum). Also, in the most-reacted spectrum in sample B (yellow), there is a considerably larger shoulder related to unreacted materials compared to the same spectrum in sample A. So, these results generally suggest that the amount of unreacted silica is higher in sample B, which correlates well with the lower gel Si/Al ratio observed in this sample.

Another potentially important difference between the two samples lies in the sharpness of the main Si−O−T bands observed in the cluster spectra. Sample A shows a markedly broader peak than sample B, which suggests that the geopolymer gel produced by gradual alumina release is composed of gel phases with a wider range of local Si/Al environments, while, in sample B, this band is sharper, meaning that Si and Al are distributed more evenly in the gel.

The homogeneity of geopolymer gels can also be investigated by chemical imaging based on infrared microscopy data. In Figure 7, the wavenumber corresponding to the highest intensity between 920 cm^{-1} and 1000 cm^{-1} (i.e., the geopolymer Si−O−T band region) is color-coded and plotted as a function of the spatial coordinates on the sample.

Figure 7 shows that there is a marked difference in the degree of homogeneity of geopolymer gels between the two samples. The presence of more regions in the chemical map with similar colors means that the Si−O−T peaks at each point are more similar to each other, corresponding to a more uniform gel. Conversely, more regions with the colors close to the limiting borders (yellow or black) means a wider distribution of main peak positions and, consequently, a more heterogeneous gel. Thus, sample B, which shows less distribution of colors in its peak position map, is more homogeneous. This correlates well with the observations based on the HCA data and the cluster spectra peak widths, and indicates that the faster release

(47) Shoval, S.; Boudeulle, M.; Yariv, S.; Lapides, I.; Panczer, G. *Opt. Mater.* **2001**, *16*, 319.

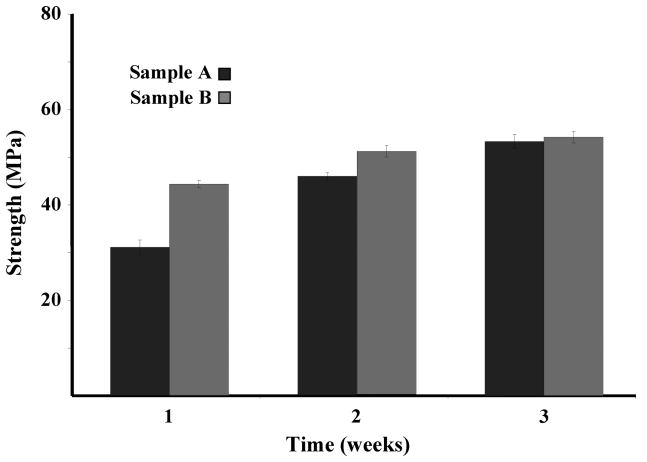

Figure 8. Compressive strength evolution of samples A and B. Data represent the average of three tests, with error bars showing ±1 standard deviation.

of alumina corresponds to the formation of a more homogeneous gel. It is still not known whether geopolymer gel homogeneity is an advantage for a binder, in terms of performance or durability; however, it is believed that the main band position of a well-reacted fly ash geopolymer gel should appear close to 960 cm^{-1}.[31] Therefore, the fast-alumina-release sample (B), which shows fewer regions with colors close to yellow or black, should contain a more reacted geopolymer gel.

As shown in Figure 4, in the fast alumina release sample (sample B), there is enough dissolved alumina available to take part in the early stages of the reaction and shift the Si−O−T band to lower wavenumbers; however, there is also enough silica available to contribute to gel formation and shift the band position quickly back to higher wavenumbers. These changes in the forming gels happen fast enough to lead to mixing of the Al-rich and Si-rich gel components, resulting in a more homogeneous binder on a length scale of a few tens of micrometers, as observable by SR-FTIR. However, in the slow-alumina-release sample (sample A), Al-rich gel formation followed by the growth of a Si-rich gel occurs very slowly, and the slow changes in gel formation mechanism give enough time for the newly formed gels to stabilize and condense by themselves, resisting further structural evolution or intermixing and resulting in a more heterogeneous binder.

3.4. Mechanical Strength. The results of compressive strength testing of geopolymer mortars (Figure 8) show that alumina dissolution rate has a significant effect on the mechanical strength development of geopolymer gel binders. The strengths achieved are approximately comparable to the expected strength of a standard portland cement-based mortar at similar ages of curing, although the strength development of sample A is rather slow, compared to most portland cement mortars.

Although sample B, with faster alumina release from the sodium aluminate precursor, shows better strength results in the first two weeks, the strength development of this sample becomes very slow after the first week. On the other hand, sample A, with slow alumina release, makes a weaker geopolymer at the beginning, but its strength development continues for a longer period of time, and the strength of the sample after 3 weeks is very similar to that of sample B.

It is believed that the contribution of aluminum to gel structure development in the early stages of the reaction plays an important role in the initial strength development of geopolymers, because the gel begins to cross-link and generate mechanical integrity. However, the contribution of silica in the later stages of gel growth is also known to be critical in strength development. Fernández-Jiménez et al.[11,17] have analyzed the mechanical strengths of fly-ash-derived geopolymers, as a function of the relative amount of silica in $Q^4(4Al)$ environments versus $Q^4(3Al) + Q^4(2Al)$ environments in geopolymer gels. They concluded that the mechanical strength of geopolymers starts to increase during the formation of the Al-rich aluminosilicate gel at low $[Q^4(3Al) + Q^4(2Al)]/Q^4(4Al)$ ratios, but that any further increase in mechanical strength is the result of silicon-enriched aluminosilicate gel formation, and higher final strength results were achieved at higher $[Q^4(3Al) + Q^4(2Al)]/Q^4(4Al)$ ratios. The data presented here are in general agreement with these observations, although the analysis conducted here is presented on the basis of infrared rather than nuclear magnetic resonance data, so the individual $Q^4(n\text{Al})$ connectivity types are not explicitly distinguished.

4. Conclusions

The effect of alumina release rate from precursor materials on the formation mechanism of geopolymer gels has been investigated. Synchrotron radiation-based infrared microscopy (SR-FTIR) data processed via hierarchical clustering analysis clarify the degree of homogeneity in geopolymer gels and provide a more detailed understanding of the differences in geopolymer gel structure induced by different rates of alumina release, which are not evident from traditional spatially resolved infrared spectroscopic analysis. It is only via the use of a high-intensity synchrotron light source that spatially resolved Fourier transform infrared (FTIR) spectroscopy of complex heterogeneous samples such as geopolymers becomes accessible.

A fast alumina release rate from geopolymer precursors provides dissolved alumina species that are readily available in solution to participate in geopolymer gel formation. Therefore, a faster geopolymerization reaction occurs in this case (i.e., faster formation of Al-rich gel followed by Si-rich gel), and more aluminum will eventually participate in the gel network. These rapid initial changes in the geopolymer gel network lead to better mixing of the forming gels, and a more homogeneous geopolymer gel results. On the other hand, the availability of a greater amount of dissolved alumina species in the early stages of the reaction hinders silica dissolution by sorption of dissolved alumina onto silica particles. This hinders silica dissolution, and, although the high rate of alumina participation in the gel network leads to high early strength of this binder, the lack of available silicon impedes further strength development. A slow alumina release rate reduces

this sorption and, therefore, provides more-rapid and more-extensive silica dissolution. However, in this case, it takes time for enough aluminum to become available to make a stable Al-rich gel, while silica dissolves and is readily available in the solution. Therefore, overall, the final geopolymer gel will have relatively less Al participation in its network and a more heterogeneous gel structure.

Acknowledgment. This work was funded in part by a studentship provided to A.H. by the Centre for Sustainable Resource Processing through the Geopolymer Alliance, and in part by the Australian Research Council (including partial support through the Particulate Fluids Processing Centre). We gratefully acknowledge the assistance of Dr. Mark Tobin and Dr. Ljiljana Puskar of the Australian Synchrotron. This research was undertaken on the BL8 (Infrared Spectroscopy) beamline at the Australian Synchrotron, Victoria, Australia. The views expressed herein are those of the authors and are not necessarily those of the owner or operator of the Australian Synchrotron.